Magnetic field influence on the spin-Peierls instability in the quasi-one-dimensional magnetostrictive XY model: Thermodynamical properties

Raimundo Alexandre Tavares de Lima
Centro Brasileiro de Pesquisas Físicas, Conselho Nacional de Desenvolvimento Científico e Tecnológico, Rua Xavier Sigaud 150, 22290 Rio de Janeiro, Brazil and Departamento de Física, Universidade Federal de São Carlos, Via Washington Luiz Km 235, São Carlos, São Paulo, Brazil

Constantino Tsallis
Centro Brasileiro de Pesquisas Físicas, Conselho Nacional de Desenvolvimento Científico e Tecnológico, Rua Xavier Sigaud 150, 22290 Rio de Janeiro, Brazil

(Received 13 May 1982)

We study in detail, within the adiabatic approximation for the structural degrees of freedom and on exact grounds for the magnetic ones, the $d=1$ magnetostrictive spin-$\frac{1}{2}$ XY model in the presence of an external magnetic field along the z axis. We calculate the specific heat, magnetization, isothermal susceptibility, and the structural order parameter and spectrum (including the sound velocity). The system presents, in temperature-field space, three structurally different phases: the uniform (U), the dimerized (D), and the modulated (M) phases (the latter can be either commensurate or incommensurate with the other two). The critical frontiers U-D and U-M are of the second-order type while the D-M one is of the first-order type; all three join at a Lifshitz point. The U-M frontier presents a new type of multicritical point on which the frozen structural wave vector vanishes. The phase diagram is quite anomalous for high values of the elastic constant. Several other effects are predicted. The present theory is expected to be applicable to substances like TTF-BDT [tetrathiafulvalinium bis-*cis*-(1,2-perfluoromethylethylene-1,2-dithiolate)-metal], TTF-BDS [tetrathiafulvalinium bis-*cis*-(1,2-perfluoromethylethylene-1,2-diselenolato)-metal], MEM(TCNQ)$_2$ (N-methyl-N-ethyl-morpholinium ditetracyanoquinodimethanide), and eventually the alkali-metal tetracyanoquinodimethanides (TCNQ).

I. INTRODUCTION

In the last decade a considerable amount of work has been dedicated to the study of the so-called spin-Peierls instability (SPI) (for an excellent recent review see Bray *et al.*[1]), which induces structural phase transitions in systems that are quasi-one-dimensional in magnetic interactions although three dimensional in crystalline interactions. Typically, the systems present a *uniform* (U) phase (referred to as the *disordered* one from Landau's standpoint, corresponding to a system of atoms equally spaced along the chain) at high temperatures and a more complex phase (referred to as the *ordered* one) at low temperatures; this phase can be structurally dimerized (D phase) or can present complex structural modulations (M phase) depending on external parameters such as the magnetic field.[2–5] The structure of the M phase might be either commensurate or incommensurate[6–9] with that of the U phase; in any case, the problem is quite analogous to that of systems exhibiting Peierls instability.[7,10–12] The spin-Peierls type of structural phase transition has been exhibited on several substances, particularly on the TTF-BDT [tetrathiafulvalinium bis-*cis*-(1, 2-perfluoromethylethylene-1, 2-dithiolate)-metal] and TTF-BDS [tetrathiafulvalinium bis-*cis*-(1, 2-perfluoromethylethylene-1, 2-diselenolato)-metal] compounds[4,13–17] $\{(TTF)^+$-$[MX_4C_4(CF_3)_4]^-$, with $(M,X)=$(Cu,S), (Au,S), and (Cu,Se)$\}$ and A^+-(TCNQ)$^-$ [A^+-tetracyanoquinodimethanide,[18–24] with A^+ equal to Na^+, K^+, Rb^+, Cs^+, and NH_4^+; within certain restrictions we could include herein A equal to $MEM_{1/2}$ (Refs. 25–28), NMP (Ref. 29), and TTF (Ref. 30), where MEM^{2+} is N-methyl-N-ethyl-morpholinium and NMP is N-methyl-phenazinium], through magnetic susceptibility,[13,18,21,25,27,29] electrical conductivity,[18–20,22,25,29] specific heat,[15,27,29,30] magnetization,[14,17] latent heat,[18] optic proper-

ties,[20,22] x-ray,[14] neutron scattering,[14,17] and EPR (Refs. 13 and 18) experiments. The theoretical approaches to this phenomenon have been performed through the use of the magnetostrictive quantum XY (Refs. 2,3,5,31–37) and Heisenberg[3,7,34,38–45] models; the former, although less frequently realistic, presents the advantage of being exactly solvable with respect to the magnetic degrees of freedom. For both models, and more particularly for the Heisenberg model, preliminary or detailed discussions have been performed concerning various quantities such as entropy,[38] specific heat,[3,38,45] magnetization,[34,38] magnetic susceptibility,[3,32,38,42,44,45] and structural order parameter,[3,11,32,35,36,39–41] as well as the influence, on some of them, of an external magnetic field[2,3,10,34,38,40,43,44] and of an external stress.[2,46]

Let us now concentrate on the magnetostrictive spin-$\frac{1}{2}$ XY model where the magnetic coupling constants are assumed to depend only on the mean distances between spins (adiabatic approximation[47]), i.e., the structural fluctuations are neglected; this assumption is expected to be acceptable if we take into account that the system is three dimensional with respect to the crystalline degrees of freedom. Pincus[31] showed that an XY antiferromagnetic chain is, at vanishing temperature, unstable with respect to dimerization, Beni and Pincus[32] exhibited next that this instability induces a second-order phase transition between the U and D phases, *under the assumption that no other phases have to be considered.* Dubois and Carton[33] proved next that, at the critical temperature T_c and coming from high temperatures, there appears a structural order which indeed is a *dimerization.* Finally, in a recent paper[36] we have exhibited that *below* T_c down to $T=0$, *no contributions to the structural order appear other than the pure dimerization one;* the same statement seems to be true[37] in the presence of an XY coupling anisotropy.[33,35]

If a magnetic field $\vec{H}$ (perpendicular to the XY plane) is applied to the system, important modifications appear in the equilibrium configuration, as the wave vector q_c characterizing the "frozen" structure might no longer be that which corresponds to a dimerization, and consequently phase transitions toward a new phase, namely the M phase, might occur. The magnetic field dependence of q_c has already been detected both theoretically[2,3,5] and experimentally[4]; however, the available discussions can be considered as preliminary. Within this respect we have recently[5] presented the complete phase diagram in the T-H space (all three U, D, and M phases) where two special points clearly appear, one of them being a Lifshitz point, the other one, referred to as *starting point,* has a nature which we attempt to elucidate herein (Sec. IV). Furthermore, in Sec. II we present all the details concerning this phase diagram; the influences of T, H, and the harmonic and anharmonic elastic constants on the dimerization order parameter (Sec. III) and on the specific heat, magnetization, isothermal magnetic susceptibility, sound velocity, and relevant optic frequency (Sec. V), are discussed as well.

II. UNIFORM CHAIN

Let us consider a cyclic linear chain (with a fixed lattice parameter equal to unity) of spins $\frac{1}{2}$ whose magnetic contribution to the Hamiltonian is given by

$$\mathcal{H}_m=-\sum_{j=1}^{2N} J_j(S_j^x S_{j+1}^x+S_j^y S_{j+1}^y)-\mu H\sum_{j=1}^{2N} S_j^z , \tag{1}$$

where μ is the elementary magneton, $H\geq 0$ by convention, and $\{J_j\}$ are local exchange integrals, and where, for future convenience, we have considered an even number of spins. Through the Jordan-Wigner transformation[48,49]

$$a_j=\left[\prod_{i=0}^{j-1} 2S_i^z\right]S_j^+ , \tag{2}$$

we may introduce pseudofermion (spinless magnetic excitations) creation ($a_j^\dagger$) and annihilation (a_j) operators, and rewrite the Hamiltonian as follows:

$$\mathcal{H}_m=-\tfrac{1}{2}\sum_{j=1}^{2N} J_j(a_j^\dagger a_{j+1}+a_{j+1}^\dagger a_j) +\mu H\sum_{j=1}^{2N} a_j^\dagger a_j-N\mu H , \tag{3}$$

where the additive term comes from the transformation

$$S_j^z=\tfrac{1}{2}-a_j^\dagger a_j . \tag{4}$$

By introducing next the Fourier-transformed quantities

$$b_k=\frac{1}{\sqrt{2N}}\sum_{j=1}^{2N} e^{ijk}a_j \quad (-\pi<k\leq\pi) \tag{5}$$

and

$$J_q=\frac{1}{2N}\sum_{j=1}^{2N} e^{ijq}J_j \quad (-\pi<q\leq\pi) , \tag{6}$$

the Hamiltonian becomes

$$\mathcal{H}_m=\mathcal{H}_0+V , \tag{7}$$

where

$$\mathcal{H}_0 \equiv |J_0| \left[\sum_k \epsilon_k b_k^\dagger b_k - Nh \right] \tag{8}$$

(this contribution is the only one in the uniform phase) and

$$V \equiv |J_0| \sum_{q\neq 0} \sum_k \Lambda_{kq} b_k^\dagger b_{k-q} , \tag{9}$$

with

$$\epsilon_k \equiv h - \cos k , \tag{10}$$

$$h \equiv \mu H / |J_0| , \tag{11}$$

$$\Lambda_{kq} \equiv -\frac{1}{2} \frac{J_q}{|J_0|} (e^{ik} + e^{i(q-k)}) . \tag{12}$$

The present treatment holds for both $J_0 > 0$ and $J_0 < 0$. However, strictly speaking, Eq. (8) is correct as it stands only for $J_0 > 0$; for $J_0 < 0$, one can introduce a description in terms of holes (instead of particles[49]) and verify that the Hamiltonian remains equivalent to that of Eq. (8), except for the sign of the magnetic field.

Let us now calculate the magnetic contribution F_m to the free energy of the system by treating V as a perturbation to $\mathcal{H}_0$ within the temperature-dependent Green's-function framework[50]; we obtain

$$F_m = F_0^1 + F_2^{(1)} + F_4^{(1)} + \cdots , \tag{13}$$

where $F_0^{(1)}$ is the magnetic free energy associated with $\mathcal{H}_0$, [the superscript (1) has been introduced for future convenience, and refers to the fact that the crystalline unit cell under consideration contains only *one* atom], symmetry excludes odd-order terms, and

$$F_j = -\frac{k_B T}{j!} \left[\frac{-1}{\hbar} \right]^j \int_0^{\hbar/k_B T} d\tau_1 \cdots \int_0^{\hbar/k_B T} d\tau_j \langle T_\tau [V_{\rm int}(\tau_1) \cdots V_{\rm int}(\tau_j)] \rangle_{\rm con} \quad (j = 2,4,\ldots) . \tag{14}$$

where T_τ is the chronological operator, the thermal average is denoted by angular brackets, whose subscript "con" denotes that only connected diagrams are to be considered, and

$$V_{\rm int}(\tau) = e^{\mathcal{H}_0 \tau/\hbar} V e^{-\mathcal{H}_0 \tau/\hbar} . \tag{15}$$

In the expansion (13) we shall retain only the first two terms ($F_2^{(1)}$ corresponds to a simple two-vertex ring diagram) as we are presently interested only in the detection of the structural mode (characterized by its wave vector q) responsible for an eventual instability of the system; later on we shall come back to this point. We obtain, through use of the quasicontinuum limit $\sum_k \to N/\pi \int_{-\pi}^{\pi} dk$,

$$f_0^{(1)} \equiv \frac{F_0^{(1)}}{N|J_0|} = -\frac{2t}{\pi} \int_0^\pi dk \ln \left[2\cosh \left[\frac{\epsilon_k}{2t} \right] \right] \tag{16}$$

and

$$f_2^{(1)} \equiv \frac{F_2^{(1)}}{N|J_0|} = \frac{1}{\pi} \sum_{q\neq 0} \int_0^\pi dk \, |\Lambda_{kq}|^2 G(k,q) , \tag{17}$$

with

$$t \equiv k_B T / |J_0| \tag{18}$$

and

$$G(k,q) = \frac{t}{2} \sum_{\omega_n} \frac{1}{(i\omega_n - \epsilon_k)(i\omega_n - \epsilon_{k-q})} , \tag{19}$$

where $\omega_n = t\pi(2n+1)$, with $n = 0, \pm 1, \pm 2, \ldots$. Through standard complex-plane integration and use of Eq. (12), we finally obtain

$$f_2^{(1)} = -\frac{1}{2\pi} \sum_{q\neq 0} \left| \frac{J_q}{J_0} \right|^2 \int_0^\pi dk \cos^2 k \frac{\tanh(\epsilon_{k+q/2}/2t) - \tanh(\epsilon_{k-q/2}/2t)}{\epsilon_{k+q/2} - \epsilon_{k-q/2}} . \tag{20}$$

Let us now take into account the elastic contribution F_e to the free energy of the system. Unlike the case for the magnetic contribution, this one will be treated only approximately (in the adiabatic approximation; see Ref. 47) in the sense that we neglect structural fluctuations; this approach should be very crude if applied to a fully one-dimensional system, but is hopefully quite acceptable to describe substances which are three-dimensional from the structural point of view although fairly one-dimensional in the magnetic interactions. By neglecting anharmonic elastic contributions (they play a minor role as will become clear further on) we have

$$F_e=\sum_{j=1}^{2N}\frac{C}{2}(X_{j+1}-X_j)^2$$

$$=2NC\sum_q(1-\cos q)\,|X_q|^2\,, \tag{21}$$

where C is the first-neighbor harmonic elastic constant, X_j is the mean position of the jth spin (with respect to its position in the uniform phase), and

$$X_q=\frac{1}{2N}\sum_{j=1}^{2N}e^{-ijq}X_j\,. \tag{22}$$

We can now go back to the magnetic contribution. If we assume that the interaction between first-neighboring spins is characterized by an exchange integral $J(u)$ where u denotes the incremental distance (with respect to that of the uniform chain) between two spins, and expand up to the linear term (higher-order terms play a minor role as will become clear later on), i.e.,

$$J(u)=J(0)+J'(0)u\,, \tag{23}$$

we obtain the parameter J_j which appears in Eq. (1),

$$J_j=J(0)+J'(0)(X_{j+1}-X_j)\,, \tag{24}$$

and hence

$$J_q=J(0)\delta_{q,0}+J'(0)(e^{-iq}-1)X_q\,, \tag{25}$$

where we have used Eqs. (6) and (22) [we note that $J_0=J(0)$]. By substituting Eq. (25) into Eq. (20) and by taking into account Eqs. (16) and (21), we obtain the total free energy F of the system:

$$f\equiv\frac{F}{N\,|J_0|}=f_0^{(1)}+\frac{1}{2}\sum_{q\neq0}\omega_q^2\eta_q^2\,, \tag{26}$$

where

$$\omega_q^2\equiv(1-\cos q)(K-L_q)\,, \tag{27}$$

$$K\equiv\frac{C\,|J(0)|}{|J'(0)|^2}\,, \tag{28}$$

$$L_q\equiv\frac{1}{4\pi\sin(q/2)}\times\int_0^\pi dk\frac{\cos^2k}{\sin k}\times\left[\tanh\frac{h-\cos(k+q/2)}{2t}-\tanh\frac{h-\cos(k-q/2)}{2t}\right], \tag{29}$$

and

$$\eta_q\equiv2\left|\frac{J'(0)X_q}{J(0)}\right|. \tag{30}$$

The critical surface in the (t,h,k) space which

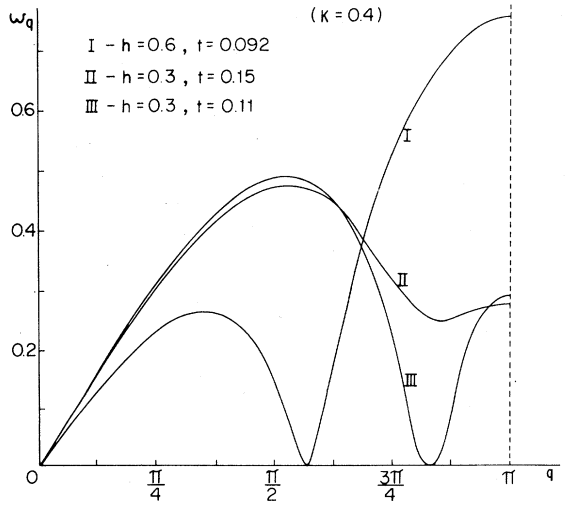

FIG. 1. Uniform-chain relevant phonon spectra associated with sets of reduced temperature t, magnetic field h, and elastic constant K. The cases I and III exhibit the trigger of incommensurate (or high-order commensurate) structural instabilities.

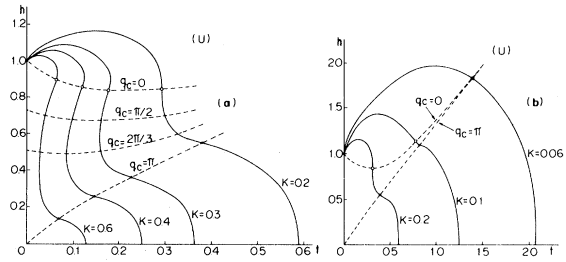

FIG. 2. Critical lines (solid) in the reduced-temperature magnetic field space; they separate, for different values of the reduced elastic constant K, the uniform (U) from the dimerized (D) and modulated (M) phases. Various constant-q_c lines (dashed) are indicated as well; those associated with $q_c=\pi$ and $q_c=0$, respectively, correspond to Lifshitz (solid dots) and "starting" (open dots) points. Note that the (a) and (b) scales are different.

separates the disordered phase (uniform chain) from ordered phases (dimerized or modulated chain) is determined by a soft-mode criterion, namely $\omega_{q_c}(t,h,K)=0$ [i.e., $K=L_{q_c}(t,h)$], where q_c is the wave vector of the first (coming from the U phase) structural mode with respect to which the system becomes unstable, i.e., q_c maximizes L_q for fixed t and h. To be more precise, $\omega_{q_c}=0$ determines the metastability limit of the U phase; this limit coincides with the critical one if and only if we are facing a second-order phase transition; this seems to be indeed the case all over the critical surface, as strongly suggested by the analysis of the particular cases treated in Sec. III [if it is so, neglecting F_4 and higher-order contributions in Eq. (13) is fully justified as long as we do not enter into the ordered phases]. We have illustrated in Fig. 1 the influence of t and h on the spectrum ω_q. In Figs. 2(a) and 2(b) we present t-h phase diagrams associated with different values of K; several constant-q_c lines are presented as well. We remark that (a) at fixed value of h and increasing t we obtain the sequence (non-U phase)—(U phase) if $h<1$, and the sequence (U phase)—(non-U phase)—(U phase) if $h>1$ and not too high; the critical frontier is *universal* (the same for all values of K) at the first-order asymptotic contribution in the limit $t\to 0$, and is given by

$$h\sim 1-t\ln(2K\sqrt{\pi t})\sim 1-(t/2)\ln t\ .$$

(b) At fixed value of t and increasing h we obtain, at intermediate temperatures, the unusual possibility of a sequence (non-U phase)—(U phase)—(non-U phase)—(U phase) if $K>K^*\simeq 0.2$; this possibility disappears for $K<K^*$. It is remarkable that the same value $K^*\simeq 0.2$ separates[37] two different regimes in the γ-t phase diagrams where γ denotes a spin-XY coupling anisotropy which can be introduced[33] in the model (in our present model $\gamma=0$). (c) The constant-q_c lines cut the h axis at points

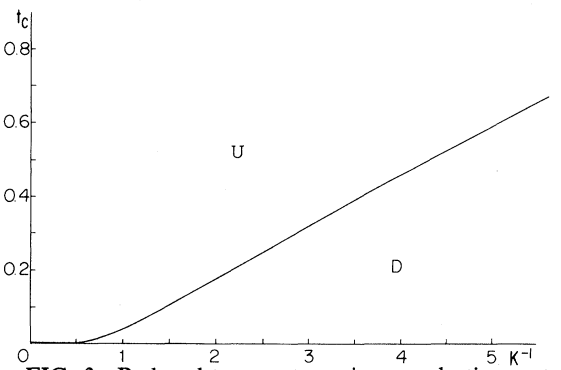

FIG. 3. Reduced-temperature—inverse-elastic-constant phase diagram associated with vanishing magnetic field; U and D, respectively, denote the uniform and dimerized phases

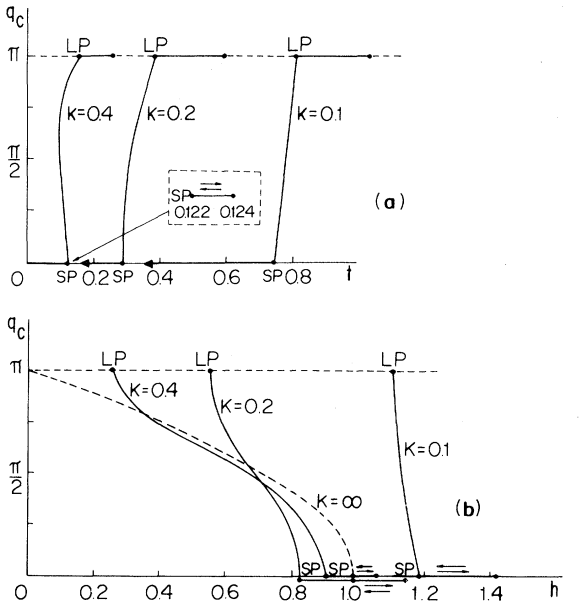

FIG. 4. Variation of the wave vector q_c (associated with the structural instability) along the critical line [q_c against the reduced temperature (a) or magnetic field (b)] associated with given values of the reduced elastic constant K; LP and SP, respectively, denote Lifshitz and "starting" points; $q_c=0$ and $q_c=\pi$, respectively, denote the uniform and dimerized phases. (b) The $K=\infty$ curve (dashed) satisfies $h=\cos(q_c/2)$; the $q_c=0$ variation of the $K=0.2$ line has been designed slightly below the abscissa only for visual purposes.

satisfying $h=\cos(q_c/2)$; this fact can be easily understood if, following along Peierls lines,[51] we remark that $q_c=2k_F$ where k_F is the Fermi wave vector of the problem [through Eq. (10), $\epsilon_{k_F}=0$ implies $h=\cos k_F$]. (d) For a given value of K, the $q_c=\pi$ and $q_c=0$ points are special ones: The former is an inflection point and corresponds (as we shall illustrate further on) to a Lifshitz point where two second-order (U-D and U-M) critical lines and one first-order (D-M) critical line converge; the latter is a peculiar one (obtained, as far as we know, for the first time and referred to hereafter as *starting* point) whose characteristics will be discussed later on (it is systematically located slightly above, in what concerns h, another inflexion point). (e) The critical temperature at vanishing magnetic field (see Fig. 3) satisfies[2,33,36,37]

$$K=\frac{1}{\pi}\int_0^{\pi/2}dk\,\frac{\sin^2 k}{\cos k}\tanh\frac{\cos k}{2t}\ , \tag{31}$$

$$K\sim\begin{cases}\dfrac{1}{\pi}\ln\dfrac{1}{t} & \text{if } t\to 0 \qquad (31')\\[2ex] \dfrac{1}{8t} & \text{if } t\to\infty \qquad (31'')\end{cases}$$

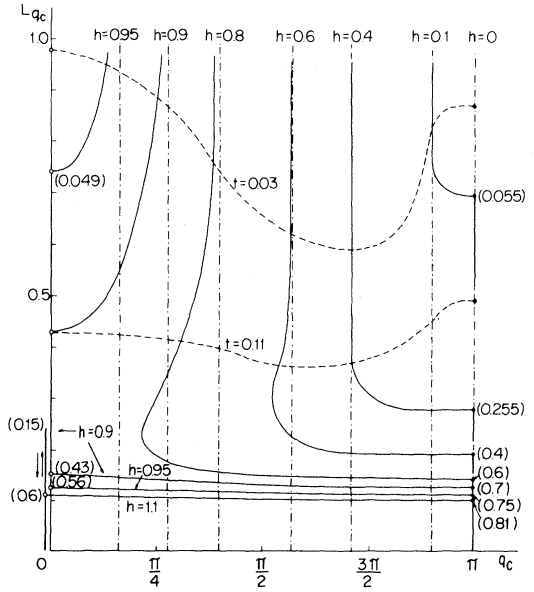

FIG. 5. Locus of the maxima of L_{q_c} with respect to q_c: several constant-field (solid) and isothermal (dashed) lines are indicated. Constant-field lines: (a) the vertical asymptotes (dotted-dashed lines) are located at $q_c = 2\arccos h$; (b) $h = 0$ ($h \to \infty$) is associated with the axis $q_c = \pi$ (axis $L_{q_c} = 0$). Isothermal lines: (a) all of them start, for $h = 0$, on the axis $q_c = \pi$ and are partially contained therein; (b) all of them are partially contained in the axis $q_c = 0$ and finish, for $h \to \infty$, at the corner $q_c = L_{q_c} = 0$; (c) the $t \to 0$ ($t \to \infty$) line corresponds to $L_{q_c} \to \infty$ ($L_{q_c} \to 0$). The solid (open) dots correspond to Lifshitz ("starting") points. The numbers between parentheses are the associated values of t.

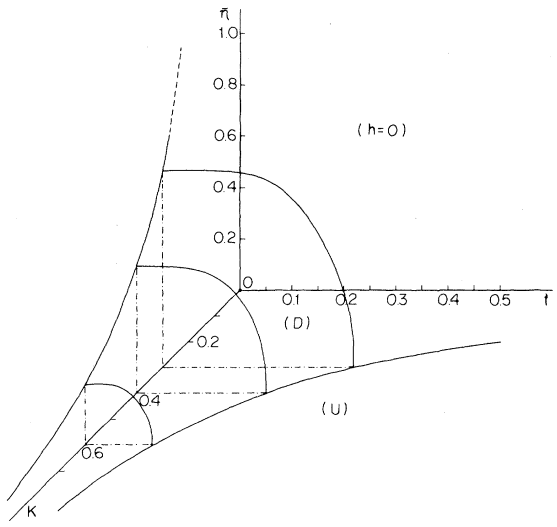

FIG. 6. Vanishing magnetic field dimerization order parameter $\bar{\eta}$ as a function of the reduced temperature t and elastic constant K; $\alpha = 0$, $\forall\delta$. The lower K is, the more important become the anharmonic effects ($\alpha > 0$) in order to avoid an unphysical growth of $\bar{\eta}$ in the low-temperature region.

Along the t-h critical line associated with a given value of K, q_c varies continuously [see Figs. 4(a) and 4(b)]. It is interesting also to analyze the main properties of the function L_q because it does not depend on K: In Fig. 5 we present the locus, in the q_c-L_{q_c} space, of the maxima of L_q with respect to q (as t and h vary). The thermal dependence of $L_\pi(t,0)$ provides the vanishing-field critical line in the t-K space (see the basal plane of Fig. 6).

III. DIMERIZED CHAIN: ORDER PARAMETER

A. Equation of state

Let us now consider the dimerized phase of our system, i.e., each unit cell of the crystal now contains two spins (hence the lattice parameter is twice its value in the uniform phase). The magnetic contribution to the Hamiltonian can be written as follows:

$$\mathscr{H}_m = -\sum_{j=1}^{N} [J(2\eta)(S^x_{2j-1}S^x_{2j} + S^y_{2j-1}S^y_{2j}) + J(-2\eta)(S^x_{2j}S^x_{2j+1} + S^y_{2j}S^y_{2j+1})] - \mu H \sum_{j=1}^{N} (S^z_{2j-1} + S^z_{2j}) , \tag{32}$$

where η is the dimerization or order parameter (the distances between neighboring spins are now alternately $1+2\eta$ and $1-2\eta$). By using, as before, the transformation (2), we obtain

$$\begin{aligned}\mathscr{H}_m &= -\tfrac{1}{2}\sum_{j=1}^{N} [J(2\eta)(a^\dagger_{2j-1}a_{2j} + a^\dagger_{2j}a_{2j-1}) + J(-2\eta)(a^\dagger_{2j}a_{2j+1} + a^\dagger_{2j+1}a_{2j})] \\ &\quad + \mu H \sum_{j=i}^{N} (a^\dagger_{2j-1}a_{2j-1} + a^\dagger_{2j}a_{2j}) - N\mu H \\ &= -\tfrac{1}{2}\sum_{k} [J(2\eta)(e^{-ik}c^\dagger_k\bar{c}_k + e^{ik}\bar{c}^\dagger_k c_k) + J(-2\eta)(e^{-ik}\bar{c}^\dagger_k c_k + e^{ik}c^\dagger_k\bar{c}_k)] + \mu H \sum (c^\dagger_k c_k + \bar{c}^\dagger_k\bar{c}_k) - N\mu H ,\end{aligned} \tag{33}$$

where $-\pi/2 < k \leq \pi/2$ and

$$c_k \equiv \frac{1}{\sqrt{N}} \sum_{j=1}^{N} \exp[i(2j-1)k] a_{2j-1} ,$$
$$\bar{c}_k \equiv \frac{1}{\sqrt{N}} \sum_{j=1}^{N} e^{i(2j)k} a_{2j} . \tag{34}$$

In order to diagonalize the Hamiltonian, we finally introduce new fermionic operators through the transformations

$$c_k = \frac{1}{\sqrt{2}}(\alpha_k + \beta_k) ,$$
$$\bar{c}_k = \frac{1}{\sqrt{2}}(\alpha_k - \beta_k) e^{i\theta_k} , \tag{35}$$

where

$$\theta_k \equiv \arctan(\bar{\eta} \tan k) \tag{36}$$

with

$$\bar{\eta} \equiv \left| \frac{J(2\eta) - J(-2\eta)}{J(2\eta) + J(-2\eta)} \right| . \tag{37}$$

Whenever Eq. (23) holds we have

$$\bar{\eta} = 2 \left| \frac{J'(0)\eta}{J(0)} \right| = \eta_\pi , \tag{37'}$$

where we have used Eq. (30). The Hamiltonian becomes

$$\mathcal{H}_m = |J(0)| \left[\sum_k (\epsilon_k^\alpha \alpha_k^\dagger \alpha_k + \epsilon_k^\beta \beta_k^\dagger \beta_k) - Nh \right] , \tag{38}$$

where

$$\epsilon_k^\alpha \equiv h - (\cos^2 k + \bar{\eta}^2 \sin^2 k)^{1/2} ,$$
$$\epsilon_k^\beta \equiv h + (\cos^2 k + \bar{\eta}^2 \sin^2 k)^{1/2} . \tag{39}$$

The free energy $F_0^{(2)}$ [the superscript (2) denotes *dimerization*] associated with this Hamiltonian is given by

$$f_0^{(2)} \equiv \frac{F_0^{(2)}}{|J(0)|N} = -\frac{2t}{\pi} \int_0^{\pi/2} dk \left[\ln \left[2 \cosh \frac{\epsilon_k^\alpha}{2t} \right] + \ln \left[2 \cosh \frac{\epsilon_k^\beta}{2t} \right] \right] . \tag{40}$$

It is straightforward to see that $\bar{\eta} = 0$ provides expression (16). The total free energy is given by

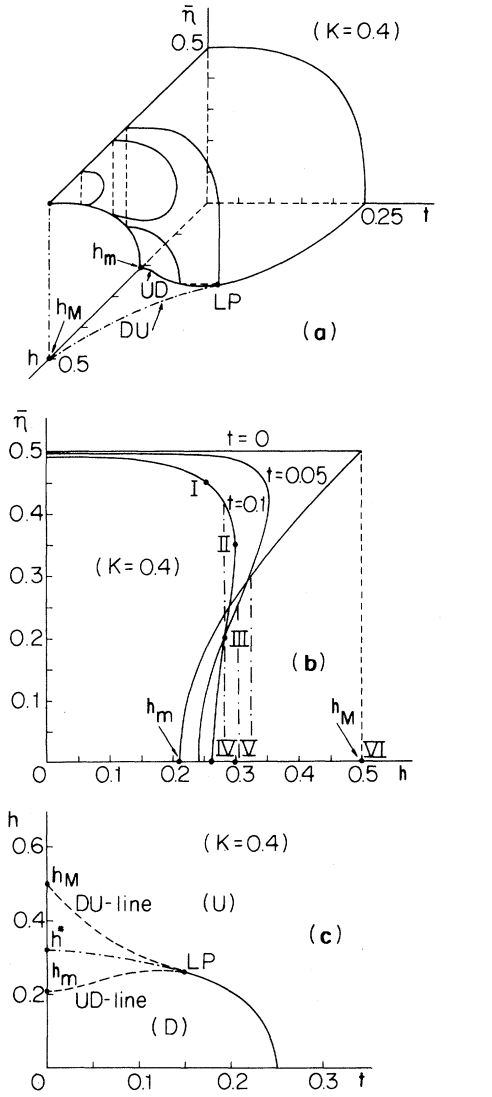

FIG. 7. Dimerization order parameter $\bar{\eta}$ as a function of the reduced temperature and magnetic field; $\alpha = 0$, $\forall\delta$. (a) The projection of the surface on the $\bar{\eta} = 0$ plane is indicated as well (dotted-dashed). (b) Isothermal lines; the dotted-dashed lines indicate the $\eta \neq 0 \leftrightarrow \eta = 0$ first-order phase transitions ($t = 0$, 0.05, and 0.1 imply $h^* = 0.325$, 0.312, and 0.285); (c) magnetic field temperature phase diagram; the solid and the dotted-dashed lines are, respectively, second- and first-order critical lines; the *UD* and *DU* lines are metastability limits. LP denotes the Lifshitz point.

$$f \equiv \frac{F}{|J(0)|N} = f_0^{(2)} + U(\bar{\eta}; \alpha, \delta) , \tag{41}$$

where $U(\eta; \alpha, \delta)$ is an elastic potential more general than $K\bar{\eta}^2$ in the sense that it may include even anharmonic contributions (characterized by the parameters $\alpha \geq 0$ and $0 < \delta \leq 1$); these contributions (which modify *absolutely nothing* in the results ob-

tained in the preceding section) play, for small values of K, an important role as we shall see in the present section (the role played by *odd* anharmonic contributions is a relatively secondary one and is neglected herein). In order to perform numerical applications we shall adopt

$$U(\bar{\eta};\alpha,\delta)=K\left[\bar{\eta}^2+\frac{\alpha\bar{\eta}^4}{1-\bar{\eta}^2/\delta^2}\right], \tag{42}$$

which provides $K\bar{\eta}^2$ if $\alpha=0$, diverges if $\bar{\eta}$ grows up to δ, and whose asymptotic expansion in the limit $\bar{\eta}\to 0$ is given by $K(\bar{\eta}^2+\alpha\bar{\eta}^4)$. To be precise let us point out that the inclusion of anharmonic terms in the variable $\bar{\eta}$ (*instead of* η) *simultaneously* covers possible departures of F_e/N from $C(2\eta)^2$ and of $J(u)$ from $J(0)+J'(0)u$ [see Eq. (23)]: this fact becomes clear if we remember the definition (37). According to our choice of a unit lattice parameter, $|\eta|$ cannot exceed $\frac{1}{2}$ (a physically acceptable F_e should diverge at this point); in the (highly probable) case that $J(u)$ [or $J(-u)$] vanishes before reaching this point, we must have $\delta=1$ because $|\bar{\eta}|$ can grow up to unity [see Eq. (37)]; in the (speculative) case in which $J(u)$ could remain finite up to $|\eta|=\frac{1}{2}$, then

$$\delta=|J(1)-J(-1)|/|J(1)+J(-1)|<1 .$$

The equation of equilibrium states $\partial f/\partial\bar{\eta}=0$ eventually admits, besides the trivial solution $\bar{\eta}=0$ (U phase), the following one:

$$\frac{\partial f_0^{(2)}}{\partial(\bar{\eta}^2)}+\frac{\partial U}{\partial(\bar{\eta}^2)}=0 . \tag{43}$$

Therefore [through use of Eqs. (40) and (42)],

$$K=\frac{A(\bar{\eta}^2;\alpha,\delta)}{2\pi}\int_0^{\pi/2}dk\frac{\sin^2k}{(\cos^2k+\bar{\eta}^2\sin^2k)^{1/2}}\times\left[\tanh\frac{\epsilon_k^\beta}{2t}-\tanh\frac{\epsilon_k^\alpha}{2t}\right], \tag{43'}$$

where

$$A(\bar{\eta}^2;\alpha,\delta)\equiv\left[1+\frac{\alpha\bar{\eta}^2(2-\bar{\eta}^2/\delta^2)}{(1-\bar{\eta}^2/\delta^2)^2}\right]^{-1} . \tag{44}$$

This equation (discussed in Secs. III B and III C) provides, for given values of K, α, and δ, the order parameter $\bar{\eta}(t,h)$ in the dimerized phase (by definition $\bar{\eta}>0$) [see Figs. 7(a) and 7(b)].

B. Vanishing temperature

The discussion of the case $t=0$ is rather complex and it is useful to separately describe six cases, respectively, associated with six different possibilities for the pseudofermion spectrum (see Fig. 8). Let us first point out that in the cases (c) and (f) no tion $\bar{\eta}\neq 0$ exists. The solution in the other four cases [(a), (b), (d), (e); see Fig. 9] satisfies

$$K=\frac{A}{\pi}\int_{k_m}^{k_M}dk\frac{\sin^2k}{(\cos^2k+\bar{\eta}^2\sin^2k)^{1/2}} ,$$

$$0\le k_m\le k_M\le\frac{\pi}{2} . \tag{45}$$

Let us first of all discuss the case $\alpha=0$ ($\forall\delta$): Equation (45) becomes

$$K=\left\{\begin{array}{ll}\left.\dfrac{F(k,(1-\bar{\eta}^2)^{1/2})-E(k,(1-\bar{\eta}^2)^{1/2})}{\pi(1-\bar{\eta}^2)}\right|_{k_m}^{k_M} & \text{if } \bar{\eta}\le 1 \quad (46)\\ \left.\dfrac{\bar{\eta}^2E(k,(\bar{\eta}^2-1)^{1/2}/\bar{\eta})-F(k,(\bar{\eta}^2-1)^{1/2}/\bar{\eta})}{\pi\bar{\eta}(\bar{\eta}-1)}\right|_{\pi/2-k_M}^{\pi/2-k_m} & \text{if } \bar{\eta}\ge 1 \quad (46')\end{array}\right.$$

where $F(x,y)$ and $E(x,y)$, respectively, denote the elliptic integrals of the first and second kind, and where $k_m=0$ and $k_M=\pi/2$ in the cases (a) and (d), $k_m=0$ and $k_M=k_c$ in the case (b), $k_m=k_c$ and $k_M=\pi/2$ in the case (e), with

$$k_c\equiv\arcsin\left[\frac{1-h^2}{1-\bar{\eta}^2}\right]^{1/2} . \tag{47}$$

We remark that if $h\le 1$ and $h\le\bar{\eta}$ [cases (a) and (d)], Eqs. (46) and (46') imply $\bar{\eta}(0,h)=\bar{\eta}(0,0)$ where $\bar{\eta}(0,0)$ satisfies

$$K=\begin{cases}\dfrac{K([1-\bar{\eta}^2(0,0)]^{1/2})-E([1-\bar{\eta}^2(0,0)]^{1/2})}{\pi[1-\bar{\eta}^2(0,0)]} & \text{if } K\geq\tilde{K}=\frac{1}{4} \quad (48)\\ \dfrac{\bar{\eta}^2(0,0)E\left[\dfrac{[\bar{\eta}^2(0,0)-1]^{1/2}}{\bar{\eta}(0,0)}\right]-K\left[\dfrac{[\bar{\eta}^2(0,0)-1]^{1/2}}{\bar{\eta}(0,0)}\right]}{\pi\bar{\eta}(0,0)[\bar{\eta}^2(0,0)-1]} & \text{if } K\leq\tilde{K}=\frac{1}{4} \quad (48')\end{cases}$$

where $K(x)$ and $E(x)$, respectively, denote the complete elliptic integrals of the first and second kind; $K=\tilde{K}\equiv\frac{1}{4}$ implies $\bar{\eta}(0,0)=1$; Equation (48) leads, in the limit $K\to\infty$, to $\bar{\eta}(0,0)\sim(4/e)e^{-\pi K}$; Equation (48′) leads, in the limit $K\to 0$, to $\bar{\eta}(0,0)\sim 1/\pi K$; $\bar{\eta}(0,h)$ presents two branches (see Fig. 9) which join at $h=h_M$ and we verify that $h_M\leq\bar{\eta}(0,0)$ (the equality holds if and only if $K\geq\tilde{K}$).

In the case (b), the lower branch of $\bar{\eta}(0,h)$ cuts the h axis at $h=h_m$ (see Fig. 9) which satisfies

$$K=\frac{1}{2\pi}\ln\frac{1+(1-h_m^2)^{1/2}}{1-(1-h_m^2)^{1/2}}-\frac{(1-h_m^2)^{1/2}}{\pi}\ . \quad (49)$$

Hence

$$h_m\sim\begin{cases}1-\dfrac{(3\pi)^{2/3}}{2}K^{2/3} & \text{if } K\to 0\\ \dfrac{2}{e}e^{-\pi K} & \text{if } K\to\infty\ .\end{cases} \quad (49')$$

Let us summarize by saying that the harmonic approximation is physically acceptable for $K>\tilde{K}=\frac{1}{4}$ and leads to interesting features such as the evidence of first-order phase transitions at vanishing temperature and $h=h^*$ ($h_m<h^*<h_M$). On the other hand, severe defects are present if $K<\tilde{K}$: We shall exhibit now that all the anomalies disap-

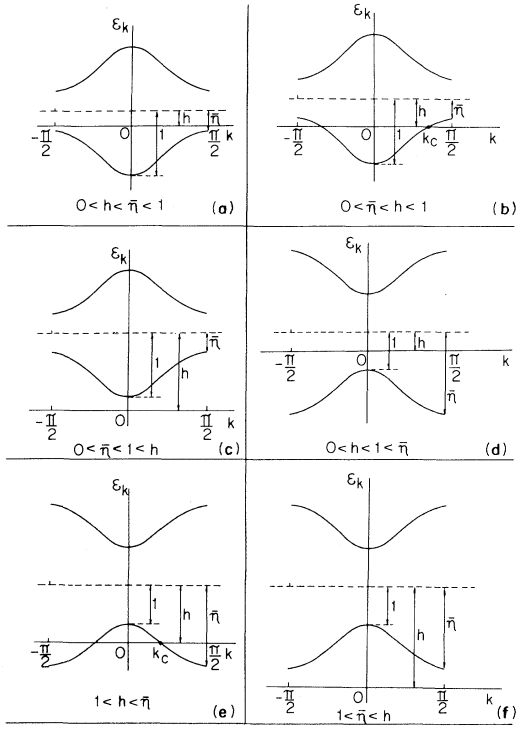

FIG. 8. Six typical possibilities for the pseudofermion spectrum. At $t=0$ only the regions with $\epsilon_k<0$ are populated. In (b) and (e) we have indicated the wave vector q_c.

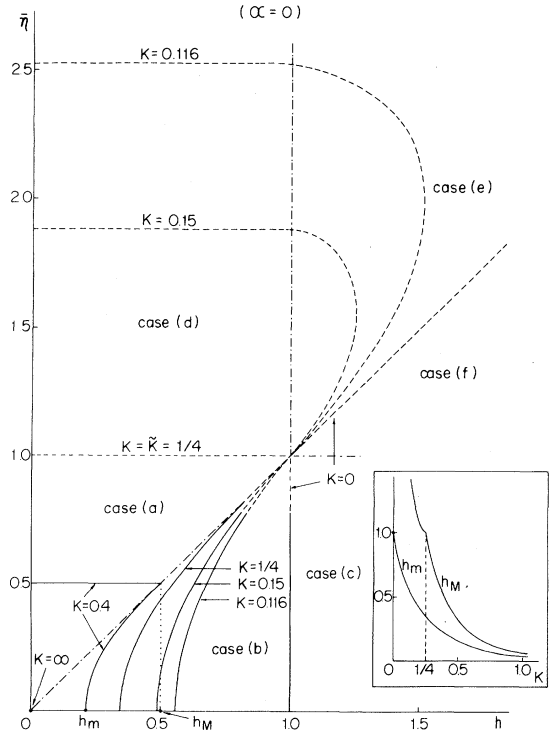

FIG. 9. Vanishing temperature dimerization order parameter associated, for different values of K, with the six cases (separated by dotted-dashed lines) for pseudofermion spectrum (see Fig. 8); $\alpha=0$, $\forall\delta$. The lines within regions where the harmonic approximation is physically unacceptable are dashed. The small figure shows the K dependence of h_m and h_M.

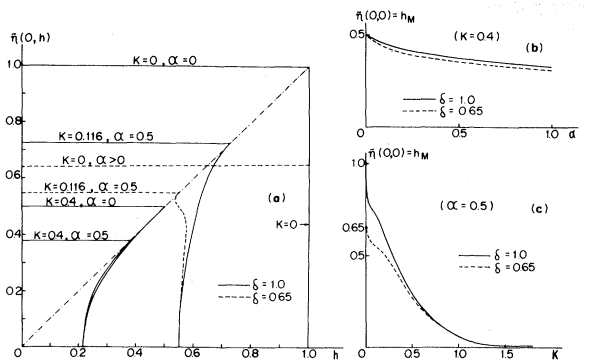

FIG. 10. Effect of anharmonicity on the vanishing temperature dimerization order parameter $\bar{\eta}(0,h)$; (a) the order parameter as a function of h for selected values of K, α, and δ; (b) $h_M=\bar{\eta}(0,0)$ as a function of α for $K=0.4$ and different values of δ; (c) h_M as a function of K for $\alpha=0.5$ and different values of δ.

pear when anharmonicity is allowed to come in ($\alpha>0$).

The $t=0$ discussion of the order parameter goes, for the anharmonic case, similarly to that of the harmonic one. The results are illustrated in Figs. 10(a)–10(c). We remark that (a) increasing α and $(1-\delta)$ lead to decreasing $\bar{\eta}(0,h)$ [in particular $\alpha\to\infty$ and/or $\delta\to 0$ imply $\bar{\eta}(0,h)\to 0$]; (b) $K=0$ leads to $\bar{\eta}(0,h)=\delta\leq 1$ for any value of α; (c) anharmonicity leads to no (large) qualitative modifications for $K>\tilde{K}=\frac{1}{4}$ ($K<\tilde{K}$); see, for example, the case $K=0.4$ ($K=0.116$) in Fig. 10(a) [Figs. 9 and 10(a)]; (d) h_m is independent from α and δ (as expected if we take into account that it concerns the limit $\bar{\eta}\to 0$) and is still given by Eq. (49); (e) $h_M=\bar{\eta}(0,0)$ strongly depends on α and δ (in particular, for $\delta=1$ it joins h_m in the limit $K\to 0$ for *any* positive value of α), and (f) within the (speculative) hypothesis $\delta<1$, unusual sequences of two first-order transitions may occur [see the case ($K=0.116$; $\alpha=0.5$; $\delta=0.65$) in Fig. 10(a)]. To conclude this section let us emphasize that anharmonicity is able to provide $\bar{\eta}\leq 1$ for *all* values of K as physically desirable.

C. Finite temperatures

We shall now go back to the complete equation of states [Eq. (43′)] and discuss the dimerization order parameter at finite temperatures; in order to simplify the numerical analysis we restrict to $K>\tilde{K}=\frac{1}{4}$, a fact which authorizes us to neglect anharmonic contributions, i.e., we adopt $\alpha=0$, and hence $A=1$ [see Eq. (44)]; the results for $K>\tilde{K}$ are qualitatively the same as long as $\alpha>0$ (and $\delta=1$ in order to concentrate on the physically relevant models). The results obtained for $h=0$ are illustrated in Fig. 6; those obtained for general values of h are illustrated in Fig. 7. We remark that for a given value of K and sufficiently high values of h, the transition ($U\leftrightarrow D$) becomes of the first order: The special point [characterized by (t_L,h_L)] which separates the second-order from the first-order regimes appears, within the present context, where no other structural order than dimerization is under consideration, such as a *tricritical* one (in fact, it will become clear later on that it is a Lifshitz point and therefore its nature is much closer to that of a *bicritical* one in the sense that two second-order and one first-order critical lines converge on it). From this point start two metastability lines, namely that of the U phase into the D phase (noted as the UD line and cutting the h axis at $h=h_m$) and that of the D phase into the U phase (noted as the DU line and cutting the h axis at $h=h_M$); see Fig. 7(c). The DU line is, of course, the projection of the surface $\bar{\eta}(t,h)$ on the plane (t,h) and, if prolonged with the second-order critical line, it exhibits an *inflection point* (which is precisely the Lifshitz point).

The first-order critical line runs between the UD and DU lines [see Fig. 7(c)], cuts the h axis at $h=h^*$, and is determined by the condition

$$f(t,h;\bar{\eta}(t,h))=f(t,h;0)\ . \tag{50}$$

Therefore,

$$f(0,h^*;\bar{\eta}^*)=f(0,h^*;0)\ , \tag{50'}$$

where $\bar{\eta}^*\equiv\bar{\eta}(0,h^*)=\bar{\eta}(0,0)$. This equality leads, through the use of Eq. (41) (with $\alpha=0$), to

$$[1-(h^*)^2]^{1/2}+h^*\ \mathrm{arcsin}h^*+\frac{\pi K}{2}(\bar{\eta}^*)^2 =E([1-(\eta^*)^2]^{1/2})\ , \tag{51}$$

which together with Eq. (48) determines η^* and h^*; we can verify a remarkable property, namely,

$$h^*=\sqrt{h_M h_m}\ , \tag{52}$$

where we have used the property $h_M=\bar{\eta}(0,0)$ and Eq. (49); in the limit $K\to\infty$ we obtain $h^*\sim(2\sqrt{2}/e)\,e^{-\pi K}$.

IV. MODULATED CHAIN AND STARTING POINT

Up to now we have seen that, for a given K (assumed from now on to be high enough to neglect anharmonicity), a critical frontier in the t-h space separates the U phase from the polymerized ones, namely the D phase (which occupies the low-h zone of the ordered region, and has been the specific subject of Sec. III) and the M phase (which occupies the high-h zone of the same region). In the present sec-

tion we intend to provide an analysis of the M phase, and more specifically concerning the two following points: (a) What is the structural order in the M phase, and (b) what is the order of the transition across the UM line? (Across the UD line the transition is a second-order one; see Sec. III). This discussion will also enlighten us as to the peculiar nature of the "starting point."

The full performance of this analysis demands the knowledge of the free energy as a function of an arbitrary structural order characterized by an order parameter η_q, where the wave vector q might or might not be commensurate with the first Brillouin zone associated with the uniform chain. With respect to the M phase we shall restrict ourselves to two particular cases (both commensurate), namely, the *tri*merized and *tetra*merized chains (respectively associated with "frozen" modes with wave vectors $q=2\pi/3$ and $q=\pi/2$; note that an "acoustic" mode with $q=2\pi/3$ corresponds to an "optic" mode with $q=\pi/3$). By following along the lines of Sec. III we obtain the s-merized total free energy given by[2]

$$f^{(s)}=f_m^{(s)}+f_e^{(s)}\ , \tag{53}$$

where $f_m^{(s)}$ and $f_e^{(s)}$ are, respectively, the magnetic free energy and the harmonic elastic potential given by

$$f_m^{(s)}\equiv\frac{F_m^{(s)}}{|J(0)|N}=-\frac{2t}{\pi}\sum_{r=1}^{s}\int_0^{\pi/s}dk\,\ln[1+\exp(-\epsilon_k^{(r)}/t)] \tag{54}$$

(if $s=2$, $r=1$ and $r=2$ correspond, respectively, to the previous families α and β) and

$$f_e^{(s)}\equiv\frac{F_e^{(s)}}{|J(0)|N}=\frac{C}{|J(0)|s}\sum_{r=1}^{s}(\eta_{r+1}-\eta_r)^2\ . \tag{55}$$

The trimerized ($s=3$) and tetramerized ($s=4$) cases that we have considered have the energy spectra given by

$$\epsilon_k^{(1)}=h-\left[\frac{1}{3}\sum_{r=1}^{3}(j_r^{(3)})^2\right]^{1/2}\cos\frac{\phi_k}{3}\ ,$$

$$\epsilon_k^{(2,3)}=h+\frac{1}{2}\left[\frac{1}{3}\sum_{r=1}^{3}(j_r^{(3)})^2\right]^{1/2}\left[\cos\frac{\phi_k}{3}\pm\sqrt{3}\sin\frac{\phi_k}{3}\right]\quad(s=3)\ , \tag{56}$$

$$\phi_k\equiv\arctan\frac{\left[\left[\frac{1}{3}\sum_{r=1}^{3}(j_r^{(3)})^2\right]-\left[\prod_{r=1}^{3}j_r^{(3)}\right]^2\cos^2(3k)\right]^{1/2}}{\left[\prod_{r=1}^{3}j_r^{(3)}\right]\cos 3k}\ \epsilon[0,\pi]\ , \tag{56}$$

and

$$\epsilon_k^{(1,2,3,4)}=h\pm\frac{1}{2}\left\{\frac{1}{2}\sum_{r=1}^{4}(j_n^{(4)})^2\pm\left[\frac{1}{4}\left[\sum_{r=1}^{4}(j_r^{(4)})^2\right]^2+2\left[\prod_{r=1}^{4}j_r^{(4)}\cos(4k)\right]-(j_1^{(4)}j_3^{(4)})^2-(j_2^{(4)}j_4^{(4)})^2\right]^{1/2}\right\}^{1/2}\quad(s=4)\ , \tag{56'}$$

where $j_r^{(3,4)}$ are the reduced exchange integrals. The analyses of these two cases were performed by taking in the Eqs. (56) and (56') the expansion

$$j_r^{(3,4)}=1+\frac{J'(0)}{J(0)}(\eta_{r+1}-\eta_r) \tag{57}$$

and assuming in Eqs. (55) and (57) a sinusoidal structural order parameter—this is reasonable for not too low temperatures—given by

$$\eta_r=\eta\cos(2\pi r/s+\psi)\ , \tag{57'}$$

with $r=1,2,\ldots,s$. We have used the phases $\psi=5\pi/6$ for $s=3$ and $\psi=\pi$ for $s=4$, obtained through minimization of the total free energy.

From the equilibrium condition $\partial f^{(s)}/\partial(\eta^2)=0$ and Eqs. (53)–(57') we obtain the respective equations of states for the trimerized and tetramerized configurations:

$$K=-\frac{16}{3\pi}\sum_{\alpha=1}^{3}\int_0^{\pi/3}dk\,\frac{e^{-(\epsilon_k^{(r)}/t)}}{1+e^{-\epsilon_k^{(r)}/t}}\frac{\partial\epsilon_k^{(r)}}{\partial(\eta_3^2)}\quad(s=3) \tag{58}$$

and

$$K=-\frac{8}{\pi}\sum_{\alpha=1}^{4}\int_0^{\pi/4}dk\frac{e^{-(\epsilon_k^{(r)}/t)}}{1+e^{-\epsilon_k^{(r)}/t}}\frac{\partial\epsilon_k^{(r)}}{\partial(\bar{\eta}_4^2)}\quad(s=4)\ . \tag{59}$$

The results are presented in Figs. 11(a) and 11(b). The transitions are of the second order on the *UM* line (and only there).

Let us now conjecture what happens in the *M* phase. We have seen[36] in the case $h=0$ that through the *U-D* critical point down to vanishing temperature there is no other structural order than *pure dimerization.* The same is true for $h>0$ in the whole *D* phase, as no other instability than that associated with $q=0$ (reduced Brillouin zone) is exhibited by the spectra $\omega_q(t,h,\bar{\eta}(t,h))$ and $\omega_q'(t,h,\bar{\eta}(t,h))$. At this point let us interrupt our analysis in order to indicate how the calculation of these spectra is performed. The quantities ω_q and ω_q' were obtained through a quite long but straightforward calculation of the free energy associated with Hamiltonian (1), conveniently written in the form (7), where $\mathscr{H}_0$ corresponds now to a pure dimerization (associated with the "optic" $q=0$ mode in the reduced Brillouin zone) and where V corresponds to the rest of the modes. We treat V as a perturbation to $\mathscr{H}_0$ within the temperature-dependent Green's-function framework, and obtain

$$\omega_q^2=m_q+|n_q|\quad\left[-\frac{\pi}{2}\le q<\frac{\pi}{2}\right],$$
$$\omega_q'^2=m_q-|n_q|\quad\left[-\frac{\pi}{2}\le q<\frac{\pi}{2}\right], \tag{60}$$

where

$$\begin{aligned}m_q\equiv K+\frac{1}{2\pi}\int_0^{\pi/2}dk\{&G(k,q)[\cos^2(k-\theta_{k,q})+\cos^2(k+\theta_{k,q})\\&-2\cos q\cos(k-\theta_{k,q})\cos(k+\theta_{k,q})]\\&+G'(k,q)[\sin^2(k-\theta_{k,q})+\sin^2(k+\theta_{k,q})\\&+2\cos q\sin(k-\theta_{k,q})\sin(k+\theta_{k,q})]\}\ ,\end{aligned} \tag{61}$$

$$\begin{aligned}n_q\equiv K\cos q+\frac{1}{2\pi}\int_0^{\pi/2}dk\{&G(k,q)[e^{-iq}\cos^2(k-\theta_{k,q})+e^{iq}\cos^2(k+\theta_{k,q})\\&-2\cos(k-\theta_{k,q})\cos(k+\theta_{k,q})]\\&+G'(k,q)[e^{-iq}\sin^2(k-\theta_{k,q})+e^{iq}\sin^2(k+\theta_{k,q})\\&+2\sin(k-\theta_{k,q})\sin(k+\theta_{k,q})]\}\ ,\end{aligned} \tag{61'}$$

$$G(k,q)\equiv-\tfrac{1}{4}\left[\frac{1}{\epsilon_{k+q/2}^{\alpha}-\epsilon_{k-q/2}^{\alpha}}\left[\tanh\frac{\epsilon_{k+q/2}^{\alpha}}{2t}-\tanh\frac{\epsilon_{k-q/2}^{\alpha}}{2t}\right]+\frac{1}{\epsilon_{k+q/2}^{\beta}-\epsilon_{k-q/2}^{\beta}}\left[\tanh\frac{\epsilon_{k+q/2}^{\beta}}{2t}-\tanh\frac{\epsilon_{k-q/2}^{\beta}}{2t}\right]\right], \tag{62}$$

and

$$G'(k,q)\equiv-\tfrac{1}{4}\left[\frac{1}{\epsilon_{k+q/2}^{\alpha}-\epsilon_{k-q/2}^{\beta}}\left[\tanh\frac{\epsilon_{k+q/2}^{\alpha}}{2t}-\tanh\frac{\epsilon_{k-q/2}^{\beta}}{2t}\right]+\frac{1}{\epsilon_{k+q/2}^{\beta}-\epsilon_{k-q/2}^{\alpha}}\left[\tanh\frac{\epsilon_{k+q/2}^{\beta}}{2t}-\tanh\frac{\epsilon_{k-q/2}^{\alpha}}{2t}\right]\right], \tag{62'}$$

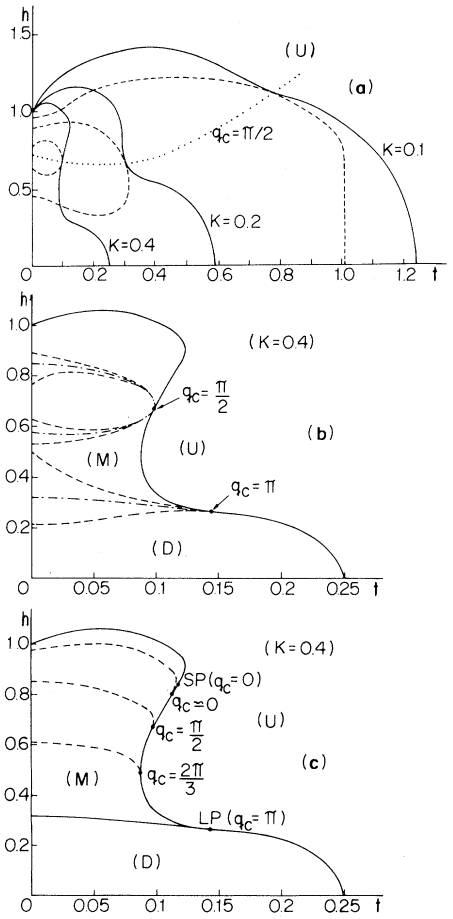

FIG. 11. (a) Critical lines (solid) in the t-h space for different values of K; the constant-q_c line (dotted) associated with the wave vector $q_c=\pi/2$ (tetramerized modulation) is indicated as well; the dashed lines indicate the $\eta=0$ metastability limit associated with the fictitious uniform-tetramerized transition. (b) Critical line for $K=0.4$; the uniform-dimerized and the (fictitious) uniform-tetramerized transitions are indicated as well (the dashed and dotted-dashed lines, respectively, denote metastability limits and the first-order critical line). (c) Phase diagram indicating the uniform (U), dimerized (D), and modulated (M) regions; the $q=2\pi/3$ and $q=\pi/2$ first-order critical lines (which possibly correspond to constant-q_M lines; see the text) are indicated (dashed) as well; the $q\simeq 0$ line is qualitative and has been included in order to characterize the nature of the starting point (SP); LP denotes the Lifshitz point.

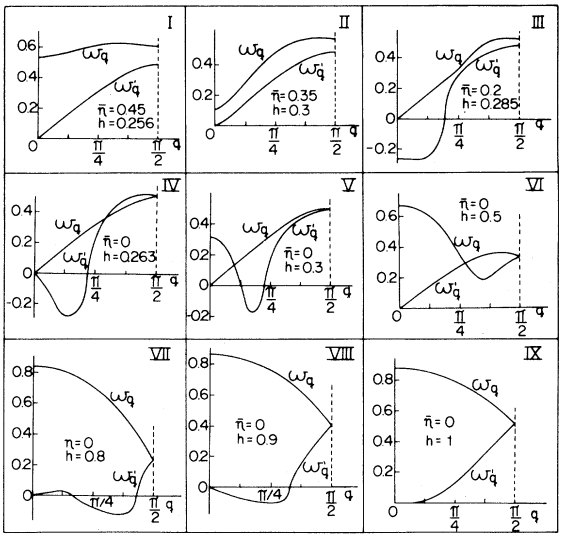

FIG. 12. Example ($K=0.4$) of the relevant phonon spectrum along an isothermal line ($t=0.1$) as a function of the magnetic field h. The cases I–VI correspond to those indicated in Fig. 7(b) (cases VII–IX are not indicated therein). In case I we are in the D phase, below the UD line (this is the type of spectrum we observed in the entire D phase, below the first-order DM line); in case II we are in the M phase, between the DM and DU lines; the DU line ($\omega_0=\omega_0'=0$) is achieved between the II and III cases; the (unphysical) case III corresponds to the location of the DM line (ω_0' presents its most negative value); the case IV corresponds to the UD line ($\omega_0'=0$); in case V we are in the M phase, above the DU line; in case VI we are in the U phase; in cases VII and VIII we are once more in the M phase; in case IX we are crossing the UM line (which, above the starting point, is simultaneously a constant-q_c line as well as a constant-q_M line with $q_c=q_M=0$).

where ϵ_k^α and ϵ_k^β are given by Eq. (39).

Let us now take up again the conjectural discussion concerning the M phase. If we neglect soliton effects as well as eventual three-dimensional magnetic ordering ones, it is plausible that in the M phase things happen similarly to the D phase in the sense that at a given point (t,h) a *unique* wave vector q_M is "frozen"; constant-q_M lines are expected to exist and they should cut the U-M line at the point associated to $q_c=q_M$ [see Fig. 11(c)]. Within an assumption of continuity the constant-q_M lines should run along the *superior* (with respect to h) branch of the phase diagram associated with the fictitious uniform-polymerized transitions [see Fig. 11(b)], and possibly coincide with their "first-order critical line" [see Fig. 11(c)]. The whole image enlightens the nature of the "starting point" and is consistent with the h dependence (at fixed t) of the spectrum $\omega_q(t,h,\bar{\eta}(t,h))$ and $\omega_q'(t,h,\bar{\eta}(t,h))$ as illustrated in Fig. 12. Let us stress that negative values of ω_q and ω_q' denote that the order parameter which has been taken into account [the dimerization parameter $\bar{\eta}(t,h)$ in the present case] *is not the appropriate one* (other wave vectors are "freezing"). In other words, it seems plausible that $\eta_q(t,h)$ is essentially a Dirac δ function of q whose evolution at $t=0$ for instance, is as follows: For $h\leq h^*$ it is located at $q=\pi$ (ex-

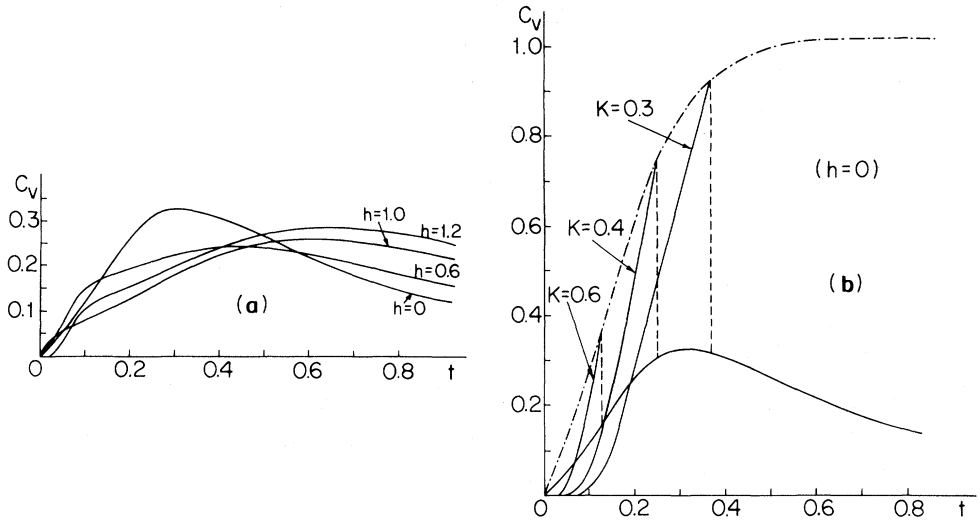

FIG. 13. Reduced specific heat (per couple of spins and in units of k_B) as a function of temperature. (a) Universal (K-independent) U-phase curves for selected values of the magnetic field; (b) vanishing magnetic field curves for selected values of the elastic constant (the dotted-dashed line indicates the locus of the maxima of C_v which occur at the respective critical points).

tended first Brillouin zone), and while h approaches unity its location monotonically runs down to $q=0$ (the amplitude should vanish as well in order to provide a second-order phase transition).

V. DIMERIZED CHAIN: OTHER PROPERTIES

Let us now turn back to the D phase in order to discuss the influence of T and H on the isochore specific heat, magnetization, isothermal magnetic susceptibility, sound velocity, and the $q=0$ "optic" frequency. We shall consider an harmonic elastic constant K high enough to neglect effects from anharmonicity.

The reduced isochore specific heat C_v is given by

$$C_v=-t\left.\frac{\partial^2 f}{\partial t^2}\right|_h , \tag{63}$$

where f is given by Eq. (41) (we recall that $\alpha=0$). We obtain, for $\bar{\eta}\equiv 0$ (U phase),

$$C_v=\frac{1}{4\pi t^2}\int_0^{\pi/2} dk\left[\frac{(h-\cos k)^2}{\cosh^2\frac{h-\cos k}{2t}}+\frac{(h+\cos k)^2}{\cosh^2\frac{h+\cos k}{2t}}\right], \tag{64}$$

$$C_v\sim\begin{cases}\dfrac{h^2+\frac{1}{2}}{4t^2} & \text{if } t\to\infty,\forall h\\ \gamma_1\dfrac{t}{(1-h^2)^{1/2}} & \text{if } t\to 0 \text{ and } h<1\\ \gamma_2\sqrt{t} & \text{if } t\to 0 \text{ and } h=1\\ \gamma_3\dfrac{e^{-(h-1)/t}}{t^{3/2}}[(h-1)^2+\gamma_4(h-1)t+\gamma_5 t^2] & \text{if } t\to 0 \text{ and } h>1\end{cases} \tag{64'}$$

($\gamma_1,\gamma_2,\ldots,\gamma_5$ are pure positive numbers), and, for $\bar{\eta}\neq 0$ (D phase),

$$C_v=\frac{1}{4\pi t^2}\left\{\int_0^{\pi/2}dk\left[\frac{(\epsilon_k^\alpha)^2}{\cosh^2(\epsilon_k^\alpha/2t)}+\frac{(\epsilon_k^\beta)^2}{\cosh^2(\epsilon_k^\beta/2t)}\right]\right.$$
$$\left.-\frac{\left[\int_0^{\pi/2}dk\left[\frac{\epsilon_k^\alpha}{\cosh^2(\epsilon_k^\alpha/2t)}-\frac{\epsilon_k^\beta}{\cosh^2(\epsilon_k^\beta/2t)}\right]\frac{\sin^2k}{(\cos^2k+\bar{\eta}^2\sin^2k)^{1/2}}\right]^2}{\int_0^{\pi/2}dk\left[\left[\frac{1}{\cosh^2(\epsilon_k^\alpha/2t)}+\frac{1}{\cosh^2(\epsilon_k^\beta/2t)}\right]-\frac{2t[\tanh(\epsilon_k^\alpha/2t)-\tanh(\epsilon_k^\beta/2t)]}{(\cos^2k+\bar{\eta}^2\sin^2k)^{1/2}}\right]\frac{\sin^4k}{\cos^2k+\bar{\eta}^2\sin^2k}}\right\}, \tag{65}$$

where ϵ_k^α and ϵ_k^β are given by Eqs. (39). Note that C_v is universal (the same for all K) in the U phase. The results are presented in Figs. 13(a) and 13(b): Their low-temperature region compares qualitatively well with the results presented in Ref. 3; let us stress, however, that the specific-heat jump may occur at a temperature *higher* than the maximum of the corresponding universal U-phase curve [see the case $K=0.3$ of Fig. 13(b)].

The reduced magnetization m is given by

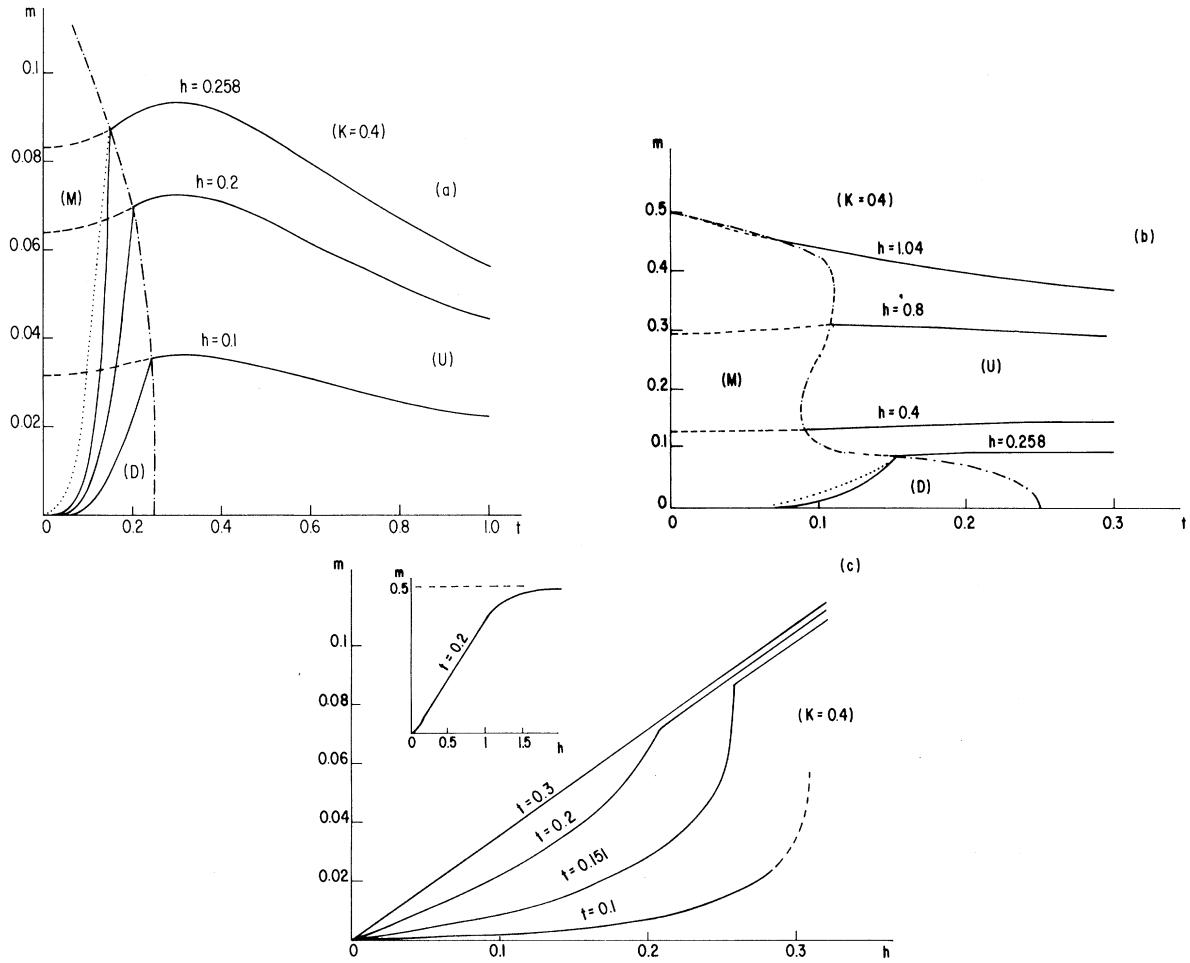

FIG. 14. Influence of the temperature t and magnetic field h on the reduced magnetization m (for $K=0.4$). Constant-field lines [(a) for $h\leq h_L\simeq 0.258$; (b) for $h\geq h_L$]: The dotted-dashed line indicates the locus of the "knees" which occur at the respective critical points and the dotted line corresponds to the first-order DM line; although graphically not visible, the $h=1.04$ line cuts the dotted-dashed line twice [see Fig. 2(a)]. Isothermal lines (c): both $t\leq t_L\simeq 0.151$ and $t>t_L$ are represented; the dashed part of the $t=0.1$ line is qualitative as it corresponds to the M phase where the equations of state are unknown; the $t=0.3$ line lies within the uniform region; in the small figure we illustrate the magnetization saturation which occurs in the high-field limit for all temperatures.

$$m=-\left.\frac{\partial f}{\partial h}\right|_t . \tag{66}$$

We obtain, for $\bar{\eta}\equiv 0$ (U phase),

$$m=\frac{1}{2\pi}\int_0^{\pi/2} dk \left[\tanh\frac{h-\cos k}{2t}+\tanh\frac{h+\cos k}{2t}\right], \tag{67}$$

$$m\sim\begin{cases}\dfrac{h}{4t} & \text{if } t\to\infty,\ \forall h \\ \dfrac{1}{\pi}[\arcsin h+\gamma_6\dfrac{t}{(1-h^2)^{1/2}}(\exp\{[-(1-h^2)^{1/2}/t]\arcsin h\} & \\ \qquad -\exp\{[-(1-h^2)^{1/2}/t]\arccos h\})] & \text{if } t\to 0 \text{ and } h<1 \\ \frac{1}{2}-\gamma_7\sqrt{t}\,e^{-(h-1)/t} & \text{if } t\to 0 \text{ and } h\geq 1\end{cases} \tag{67'}$$

(γ_6 and γ_7 are pure positive numbers), and, for $\bar{\eta}\neq 0$ (D phase),

$$m=\frac{1}{2\pi}\int_0^{\pi/2} dk \left[\tanh\frac{h-(\cos^2 k+\bar{\eta}^2\sin^2 k)^{1/2}}{2t}+\tanh\frac{h+(\cos^2 k+\bar{\eta}^2\sin^2 k)^{1/2}}{2t}\right]. \tag{68}$$

The results are presented in Figs. 14(a) and 14(b): They provide, as particular cases, situations which are compatible with those appearing in Fig. 2 of Ref. 34.

The reduced isothermal magnetic susceptibility χ is given by

$$\chi=\left.\frac{\partial m}{\partial h}\right|_t=-\left.\frac{\partial^2 f}{\partial h^2}\right|_t . \tag{69}$$

We obtain, for $\bar{\eta}\equiv 0$ (U phase),

$$\chi=\frac{1}{4\pi t}\int_0^{\pi/2} dk \left[\frac{1}{\cosh^2[(h-\cos k)/2t]}+\frac{1}{\cosh^2[(h+\cos k)/2t]}\right], \tag{70}$$

$$\chi\sim\begin{cases}\dfrac{1}{4t}\left[1-\dfrac{h^2}{4t^2}\right] & \text{if } t\to\infty,\ \forall h \\ \dfrac{1}{\pi(1-h^2)^{1/2}} & \text{if } t\to 0 \text{ and } h<1 \\ \gamma_8\dfrac{e^{-[(h-1)/t]}}{\sqrt{t}} & \text{if } t\to 0 \text{ and } h\geq 1\end{cases} \tag{70'}$$

(γ_8 is a pure positive number), and, for $\bar{\eta}\neq 0$ (D phase),

$$\chi=\frac{1}{2\pi t}\left\{\int_0^{\pi/2} dk\left[\frac{1}{\cosh^2(\epsilon_k^\alpha/2t)}+\frac{1}{\cosh^2(\epsilon_k^\beta/2t)}\right]\right. \\ \left.-\frac{1}{2}\frac{\left[\int_0^{\pi/2} dk\left[\tanh^2\dfrac{\epsilon_k^\alpha}{2t}-\tanh^2\dfrac{\epsilon_k^\beta}{2t}\right]\dfrac{\sin^2 k}{(\cos^2+\bar{\eta}^2\sin^2 k)^{1/2}}\right]^2}{\int_0^{\pi/2} dk\left[\left[\dfrac{1}{\cosh^2(\epsilon_k^\alpha/2t)}+\dfrac{1}{\cosh^2(\epsilon_k^\beta/2t)}\right]-2t\left[\tanh\dfrac{\epsilon_k^\alpha}{2t}-\tanh\dfrac{\epsilon_k^\beta}{2t}\right]\dfrac{\sin^4 k}{(\cos^2 k+\bar{\eta}^2\sin^2 k)^{1/2}}\right]}\right\}. \tag{71}$$

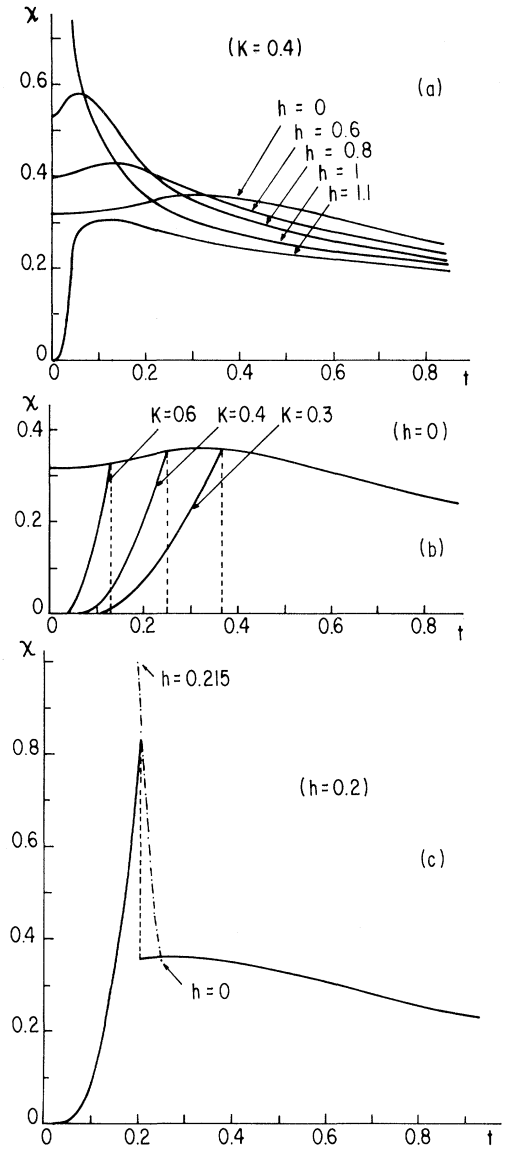

FIG. 15. Thermal behavior of the reduced isothermal magnetic susceptibility; (a) the universal (K-independent) U-phase curves for selected values of the magnetic field; (b) illustration, for selected values of the elastic constant K and vanishing magnetic field (appearance of a *discontinuity*); the dotted-dashed line represents the locus of the peaks (it suggests a divergence as the Lifshitz point is approached).

The results are presented in Figs. 15(a)–15(c). They provide, as particular cases, situations which are compatible with those appearing in Fig. 5 of Tannous and Caillé (Ref. 3); let us also remark that the curves are universal (the same for all K) in the U phase.

Finally, the reduced sound velocity v is defined through

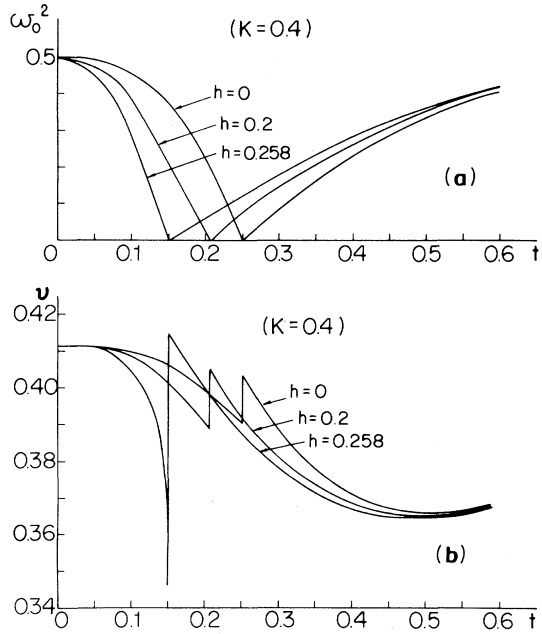

FIG. 16. Thermal dependence of the $q=0$ optical square reduced frequency (a) and the reduced sound velocity (b) for $K=0.4$ and different values of $h \leq h_L \simeq 0.258$; in the $t \to \infty$ limit ω_0 and v, respectively, saturate at $\sqrt{2K}$ and $\sqrt{K/2}$.

$$v \equiv \left. \frac{\partial \omega_q'}{\partial q} \right|_{q=0}, \tag{72}$$

where ω_q' is given by Eq. (60). The results, as well as those obtained for ω_0 (soft mode), are presented in Figs. 16(a) and 16(b).

VI. CONCLUSION

The spin-Peierls instability which occurs in magnetically quasi-one-dimensional and structurally three-dimensional systems [TTF-BDT, TTF-BDS, MEM(TCNQ)$_2$, alkali-metal TCNQ, etc.] is at the origin of a great richness of thermodynamical and dynamical properties. It seems plausible[40] that the influence of the magnetic coupling being of the Heisenberg-type, or rather, of the XY type, is a secondary one (the same is not true[35,37] if the model approaches the Ising one). On the other hand, the eventual presence of an external magnetic field (perpendicular to the XY plane in the case of an XY model) substantially modifies the physical characteristics of the problem. In the present paper we have, for the magnetostrictive spin $-\frac{1}{2}$ XY model, exactly taken into account the magnetic degrees of freedom (in the uniform and dimerized phases) but only approximatively taken into account the

structural degrees of freedom (more precisely we have neglected structural fluctuations, an approximation which should not be too crude if we consider that the system is a three-dimensional crystal; we have, furthermore, neglected eventual soliton effects).

We have extended (in what concerns the domains of variation of the temperature, magnetic field, and harmonic elastic constant) the available results[3,7,34] for the specific heat, magnetization, and magnetic susceptibility (see Figs. 13–15). Furthermore, a certain amount of interesting phenomena have been exhibited (for the first time, as far as we know). We now recall those phenomena which seem to be the most relevant among them:

(a) The system presents, in the T-H space, three structurally different phases: The uniform (U), the dimerized (D), and the modulated (M) phases. In the whole region of existence of the D phase, a *unique* wave vector q_M (namely $q_M=\pi/a$, where a is the lattice parameter of the uniform chain) characterizes the "frozen" structure. This is probably still true in the M phase in spite of the fact that q_M continuously varies (between 0 and π/a) therein, by taking values which can be commensurate or incommensurate with the Brillouin zone associated with the U phase.

(b) The first-order critical frontier which separates the D and M phases is such that the critical magnetic field increases (decreases) with temperature if the harmonic elastic constant is sufficiently small (large).

(c) The frontier which separates the U phase from the other two phases is a second-order one, and presents two special points; one of them is a Lifshitz point and corresponds to the point where the relevant wave vector q_c begins to differ from π/a (it is an inflection point of the frontier; furthermore, the first-order D-M frontier joins precisely there the second-order frontier); the other point, referred to as "starting point," exhibits a quite peculiar nature [see Fig. 11(c)] and corresponds to the point where q_c vanishes (this fact occurs at *finite* temperature). The Lifshitz and starting points monotonously approximate to each other for the decreasing harmonic elastic constant.

(d) For sufficiently high elastic constants, fixed temperature, and increasing magnetic field, it is possible to observe [see Fig. 2(a)] the unusual phase sequence nonuniform-uniform-nonuniform-uniform; for all values of the elastic constant, intermediate values of the magnetic field and increasing temperature, the sequence which occurs is U-M-U.

(e) The thermal dependence of the sound velocity presents a gap at the U-D critical points (possibly at the U-M critical points as well) which grows considerably in the presence of an external magnetic field. Less spectacular effects (softening) are predicted for the $q=0$ "optic" frequency (some experimental indications for this softening are already available[14]).

Experimental evidence of the above effects would be very welcome.

As a final conclusion let us present a few numerical comparisons of the present theory with other available theoretical and experimental results:

(i) The location of the Lifshitz point is characterized by $T_L/T_C(H=0)$; experimental values [obtained for TTF-Au-BDT, TTF-Cu-BDT, and MEM(TCNQ)$_2$] range between about 0.65 and 0.8 (see Ref. 1 and particularly Fig. 24 therein); theories from Bray[7] and Bulaevskii *et al.*[34] provide 0.54, and that from Cross[7] provides 0.77; the present treatment yields values which range from 0.59 to 0.68 while the reduced (harmonic) elastic constant K decreases from 0.6 to 0.06.

(ii) The location of the Lifshitz-point critical magnetic field H_L is characterized by $H_L/T_c(H=0)$; this quantity is experimentally determined [for the same three substances in (i)] to be 10.5 ± 0.6 (Ref. 1), with H given in kilo-oersteds and T in degrees kelvin; the Bray[7] and Bulaevskii *et al.*[34] theories provide 11.2 and the Cross[7] theory provides 10.3. In terms of the present reduced variables we have

$$H_L/T_c(H=0)=(k_B/\tilde{g}\mu_B)(h_L/t_c(h=0))$$
$$=7.47h_L/t_c(h=0)\ ,$$

where we have used the gyromagnetic ratio $\tilde{g}=2$ (EPR results[13] for TTF-Cu-BDT yield $\tilde{g}$ ranging between 2.0016 and 2.0151) and Bohr magneton μ_B; $H_L/T_C(H=0)$ varies from 7.4 to 8.0 while K increases from 0.3 to 0.6.

(iii) It is both experimentally and theoretically found that, in the limit $H\to0$,

$$\frac{T_c(H=0)-T_c(H)}{T_c(H=0)}\sim\lambda\left[\frac{\mu_B H}{k_B T_c(H=0)}\right]^2\ ,$$
$$\lambda>0\ .$$

λ is theoretically determined to be 0.44 [Refs. 7 (Bray) and 34] or 0.36 [Ref. 7 (Cross)]; our treatment provides $\lambda\simeq0.9$. A first analysis[1] of the experimental data [relative to the same three substances in (i)] was compatible with our value, while further analysis[1] was more compatible with the other two values.

(iv) The vanishing-field isothermal magnetic susceptibility also enables severe comparisons: for example, in the region of the "knee at T_c, namely the quantity

$$d[\chi(T)/\chi(T_c)]/d[T/T_c]\,|^{D}_{T=T_c}\,.$$

Experimental results (Fig. 10 of Ref. 1) for TTF-Cu-BDT provide the value 2.7; in our treatment this quantity presents, in the neighborhood of $K=0.4$, a maximum value of about 2.5 (its value is about 2 for both $K=0.3$ and 0.6).

(v) The vanishing-field derivative $d\chi/dT\,|^{U}_{T=T_c}$ could, in principle, be negative; however, typically it is positive; in this case by further increasing the temperature ($T>T_c$), χ achieves a maximum $\chi_{\max}$ at $T=T_{\max}$; the experimental evidence (Fig. 10 of Ref. 1) on TTF-Cu-BDT provides a ratio $T_{\max}/T_c\simeq 4$; in our treatment this ratio is, for $K=0.6$, 2.5 and achieves the value 4 for $K>0.6$.

(vi) In what concerns the ordinates of graphs χ vs T (vanishing magnetic field), it is possible to extrapolate, in the limit $T\to 0$, the thermal dependence of χ in the *uniform* phase, thus obtaining $\chi(T=0;\text{extrap})$; the already-mentioned experiment (Fig. 10 of Ref. 1) on TTF-Cu-BDT provides a ratio $\chi_{\max}/\chi(T=0;\text{extrap})\simeq 1.4$; this ratio equals, within the present treatment, the value 1.1 in the neighborhood of $K=0.4$; within the Beni and Pincus approach[32] the result is similar.

Similar to the other theoretical proposals available in the literature, the present one is not strictly capable of *numerically* reproducing, *with a single set of parameters,* a large variety of experimental results; this is not surprising if we take into account its intrinsic simplicity. However, we have exhibited that, with values of K (quantity related to a subtle one, namely the space variation of the exchange integral) ranging from, for example, 0.4 to 0.6, an overall description is possible which numerically is acceptable and which qualitatively is no doubt quite satisfactory. This fact raises (at least in *our* minds) the hope that most of the predictions provided by the present theory (particularly points (a)—(e) in this section) can be verified in nature.

Note added in proof. Very recent experimental results [J. A. Northby, H. A. Groenendijk, L. J. de Jongh, J. C. Bonner, I. S. Jacobs, and L. V. Interrante, Phys. Rev. B 25, 3215 (1982); J. A. Northby, F.J.A.M. Greidanus, W. J. Huiskamp, L. J. de Jongh, I. S. Jacobs, and L. V. Interrante, J. Appl. Phys. 53, 8032 (1982)] provide a quite clear suggestion of the existence in nature of the phase diagram indicated in Fig. 11(c) (particularly with respect to the neighborhood of the Lifshitz point).

ACKNOWLEDGMENTS

One of us (C.T.) has the pleasure of acknowledging extremely enlightening discussions with J. C. Bonner as well as fruitful comments from I. S. Jacobs, L. J. de Jongh, J. A. Northby, and D. Bloch.

[1]J. W. Bray, L. V. Interrante, I. S. Jacobs, and J. C. Bonner, in *Extended Linear Chain Compounds,* edited by J. S. Miller (Plenum, New York, 1982), Vol. III, p. 353.

[2]C. Tsallis, doctoral thesis, Université Paris, Orsay, 1974 (unpublished); C. Tsallis and L. de Séze, Ferroelectrics 14, 661 (1976).

[3]J. H. H. Perk, H. W. Capel, M. J. Zuilhof, and Th. J. Siskens, Physica 81A, 319 (1975); C. Tannous and A. Caillé, Can. J. Phys. 57, 508 (1979); Y. Lépine, C. Tannous and A. Caillé, Phys. Rev. B 20, 3753 (1979).

[4]I. S. Jacobs, J. W. Bray, H. R. Hart, Jr., L. V. Interrante, J. S. Kasper, D. Bloch, J. Voiron, J. C. Bonner, D. E. Moncton, and G. Shirane, J. Magn. Magn. Mater. 15-18, 332 (1980); D. Bloch, J. Voiron, J. C. Bonner, J. W. Bray, I. S. Jacobs, and L. V. Interrante, Phys. Rev. Lett. 44, 294 (1980).

[5]R. A. T. Lima and C. Tsallis, Solid State Commun. 44, 1091 (1982).

[6]S. Aubry, in *Solitons and Condensed Matter Physics,* edited by A. R. Bishop and T. Schneider (Springer, Berlin, 1978).

[7]J. W. Bray, Solid State Commun. 26, 771 (1978); M. C. Cross, Phys. Rev. B 20, 4606 (1979).

[8]A. D. Bruce and R. A. Cowley, J. Phys. C 11, 3577 (1978); 11, 3591 (1978); 11, 3609 (1978).

[9]J. Villain and M. Gordon, J. Phys. C 13, 3117 (1980).

[10]M. C. Leung, Phys. Rev. B 11, 4272 (1975).

[11]Per Bach and V. J. Emery, Phys. Rev. Lett. 36, 978 (1976).

[12]Y. Lépine and A. Caillé, Solid State Commun. 28, 655 (1978); A. Kotani and I. Harada, J. Phys. Soc. Jpn. 49, 535 (1980).

[13]I. S. Jacobs, J. W. Bray, H. R. Hart, Jr., L. V. Interrante, J. S. Kasper, G. D. Watkins, D. E. Prober, and J. C. Bonner, Phys. Rev. B 14, 3036 (1976).

[14]D. E. Moncton, R. J. Birgeneau, L. V. Interrante, and F. Wudl, Phys. Rev. Lett. 39, 507 (1977); J. S. Kasper and D. E. Moncton, Phys. Rev. B, 20, 2341 (1979).

[15]T. Wei, A. J. Heeger, M. B. Salamon, and G. E. Delker, Solid State Commun. 21, 595 (1977).

[16]E. Ehrenfreud and L. S. Smith, Phys. Rev. B 16, 1870 (1977); J. C. Bonner *et al.,* J. Appl. Phys. 50, 1810 (1979); J. N. Fields *et al., ibid.* 50, 1807 (1979).

[17]J. W. Bray, L. V. Interrante, I. S. Jacobs, D. Bloch, D. E. Moncton, G. Shirane, and J. C. Bonner, Phys. Rev. B 20, 2067 (1979).

[18]J. G. Vegter, T. Hibma, and J. Kommandeur, Chem.

Phys. Lett. 3, 427 (1969).
[19]N. Sakai, F. Shirotani, and S. Minomura, Bull. Chem. Soc. Jpn. 45, 3314 (1972).
[20]S. K. Khanna, A. A. Bright, A. F. Garito, and A. J. Heeger, Phys. Rev. B 10, 2139 (1974).
[21]J. G. Vegter and J. Kommandeur, Mol. Cryst. Liq. Cryst. 30, 11 (1975).
[22]D. B. Tanner, C. S. Jacobsen, A. A. Bright, and A. J. Heeger, Phys. Rev. B 16, 3283 (1977).
[23]M. Konno, T. Ishii, and Y. Saito, Acta Crystallogr. B 33, 763 (1977).
[24]H. Terauchi, Phys. Rev. B 17, 2446 (1978).
[25]P. I. Kuindersma, G. A. Sawatzky, and J. Kommandeur, J. Phys. C 8, 3005 (1975); 8, 3016 (1975).
[26]A. Bosch and B. van Bodegon, Acta Crystallogr. B 33, 3013 (1977).
[27]S. Huizinga, J. Kommandeur, G. A. Sawatzky, B. T. Thole, K. Kopinga, W. J. M. de Jonge, and J. Roos, Phys. Rev. B 19, 4723 (1979).
[28]H. A. Mook *et al.*, Bull. Am. Phys. Soc. 24, 507 (1979).
[29]A. J. Epstein, S. Etemad, A. F. Garito, and A. J. Heeger, Phys. Rev. B 5, 952 (1972).
[30]R. A. Craven, M. B. Salamon, G. De Pasquali, R. M. Herman, G. Stucky, and A. Schultz, Phys. Rev. Lett. 32, 769 (1974).
[31]P. Pincus, Solid State Commun. 9, 1971 (1971).
[32]G. Beni and P. Pincus, J. Chem. Phys. 57, 3531 (1972).
[33]J. Y. Dubois and J. P. Carton, J. Phys. 35, 371 (1974).
[34]L. N. Bulaevskii, A. I. Buzdin, and D. I. Komskii, Solid State Commun. 27, 5 (1978).
[35]Y. Lépine and A. Caillé, J. Chem. Phys. 71, 3728 (1979); Y. Lépine, Phys. Rev. B 24, 5242 (1981).
[36]R. A. T. Lima and C. Tsallis, Solid State Commun. 40, 155 (1981).
[37]C. Tsallis and D. M. H. da Silva, Solid State Commun. 43, 895 (1982).
[38]J. C. Bonner and M. E. Fisher, Phys. Rev. 135, A640 (1964).
[39]G. Beni, J. Chem. Phys. 58, 3200 (1973).
[40]E. Pytte, Phys. Rev. B 10, 4637 (1974).
[41]Y. Lépine and A. Caillé, J. Chem. Phys. 67, 5598 (1977).
[42]Y. Lépine, A. Caillé, and V. Larochelle, Phys. Rev. B 18, 3585 (1978).
[43]M. C. Cross and D. S. Fisher, Phys. Rev. B 19, 402 (1979).
[44]J. C. Bonner, H. W. Blöte, J. W. Bray, and I. S. Jacobs, J. Appl. Phys. 50, 1810 (1979).
[45]Y. Takaoka and K. Motizuki, J. Phys. Soc. Jpn. 47, 1752 (1979).
[46]J. W. Bray, Solid State Commun. 35, 853 (1980); I. S. Jacobs, J. W. Bray, L. V. Interrante, D. Bloch, J. Voiron, and J. C. Bonner, in *Physics in One Dimension,* edited by J. Bernasconi and T. Schneider (Springer, New York, 1981), p. 173.
[47]C. Domb, J. Chem. Phys. 25, 783 (1956); S. R. Salinas, J. Phys. C 7, 241 (1974).
[48]P. Jordan and E. Wigner, Z. Phys. 47, 631 (1928); S. Katsura, Phys. Rev. 127, 1508 (1962).
[49]E. Lieb, T. Schultz, and D. Mattis, Ann. Phys. 16, 407 (1961).
[50]A. A. Abrikosov, L. P. Gorkov, and I. E. Dzialoshinski, *Methods of Quantum Field Theory in Statistical Physics* (Dover, New York, 1963), p. 120.
[51]R. E. Peierls, *Quantum Theory of Solids* (Oxford University Press, London, 1954), p. 108.